CHALMERS
UNIVERSITY OF TECHNOLOGY

Towards an accurate estimation of heat flux distribution in metal cutting by machine learning

Citation for the original published paper (version of record):
Ertürk, A., Malakizadi, A., Larsson, R. (2023). Towards an accurate estimation of heat flux distribution in metal cutting by machine learning. Procedia CIRP, 117: 359-364.
http://dx.doi.org/10.1016/j.procir.2023.03.061

Available online at www.sciencedirect.com

ScienceDirect

Procedia CIRP 117 (2023) 359–364

www.elsevier.com/locate/procedia

19th CIRP Conference on Modeling of Machining Operations

Towards an accurate estimation of heat flux distribution in metal cutting by machine learning

Ahmet Semih Erturk*[,a], Amir Malakizadi[b], Ragnar Larsson[a]

[a]*Division of Materials and Computational Mechanics, Department of Industrial and Materials Science, Chalmers University of Technology, Göteborg SE-41296, Sweden*

[b]*Division of Materials and Manufacture, Department of Industrial and Materials Science, Chalmers University of Technology, Göteborg SE-41296, Sweden*

* Corresponding author. *E-mail address:* erturk@chalmers.se

Abstract

This study presents a machine learning-based approach for inverse identification of heat flux distribution on the rake face of the cutting tools in machining. This approach includes temperature measurements from thermocouples embedded in the tool and heat transfer finite element (FE) simulations to create the data required to train the ML model. The identified heat flux distribution is compared with the distribution from FE machining simulations for validation. The results show a clear potential to estimate the heat flux distribution in machining more efficiently by using an ML-based inverse approach.

Keywords: Heat flux; Heat transfer simulation; Inverse identification; Machine Learning; Machining; Metal cutting; Temperature

1. Introduction

Heat generation plays a significant role in machining processes due to its effects on surface integrity and tool wear. The difficulties in performing temperature measurements during machining have encouraged researchers to pursue analytical or numerical methods for the estimation of temperature at the tool-chip interface. An alternative approach is to determine the heat flux using inverse methodologies, where the experimental temperature measurements are used as a reference to identify the heat flux on the contact area. For this, the finite element method (FEM) or the finite difference method (FDM) is generally used to solve the heat transfer problem and the results are compared with the experimental results, generally measured by embedded thermocouples within the tools or workpiece material. As an example, Yvonnet et al. [1] presented an inverse approach for temperature identification. The authors performed a machining experiment and measured the temperature with a thermocouple during the operation. By using these measurements and creating a finite element (FE) model, the heat flux distribution on the rake face in 2D and the heat transfer coefficient between the tool and the environment are identified. Norouzifard and Hamedi [2], presented an inverse identification approach based on the sequential function specification (SFS) method to estimate the heat flux on the tool-chip interface at different time intervals. Combining this method with an FE model provided the possibility to estimate the temperature and the thermal contact conductance. Similarly, Brito et al. [3] used an inverse approach combining the FE simulation results with experimentation to identify the heat flux including the complex geometry of the tool-chip contact area. A more detailed estimation of heat flux is performed by Huang et al. [4], which includes the time and spatial dependency of the heat flux distribution on the rake face. Again, the inverse approach is supported by machining experiments. The FE simulations are stated as very robust, with the potential of being an online tool for heat flux estimations. Kryzhanivskyy et al. [5] included both time-dependent and spatial distribution of the heat flux on the tool surface in their FE-based inverse approach. In this study, different heat flux expressions are evaluated for the time-dependency, while the spatial distribution of the heat flux on the rake face is investigated by using an exponential function. Some of these studies investigated the heat flux in 2D, while others used a simpler machining case, neglecting the effect of the tool nose. How-

2212-8271
10.1016/j.procir.2023.03.061

ever, for a realistic heat flux estimation, the investigation should be performed in 3D, including complex cases of machining and different cutting conditions with both time-dependent and spatial distribution of heat flux.

In this study, our aim is to obtain an accurate estimation of heat flux distribution on the rake face by an ML-based inverse identification approach. This approach compares the results of FE heat transfer simulations and temperature measurements using embedded thermocouples to determine the parameters of a predefined heat flux distribution equation. An ML model is implemented to describe the relation between heat flux distribution parameters and the absolute error between simulated and experimental temperature measurements. Then, this model is used to estimate the optimum set of parameters giving the minimum error between the simulated temperatures and measurements. Compared to our previous study [6], the inverse methodology is enhanced further by adding the time-dependency of the heat flux, the chip flow direction, the effect of the tool nose and by imposing an additional constraint during the optimization process limiting the maximum temperature on the rake face based on previously reported experimental results in the literature. Additionally, a machining simulation is performed to validate the temperature distribution on the rake face obtained from the presented inverse approach.

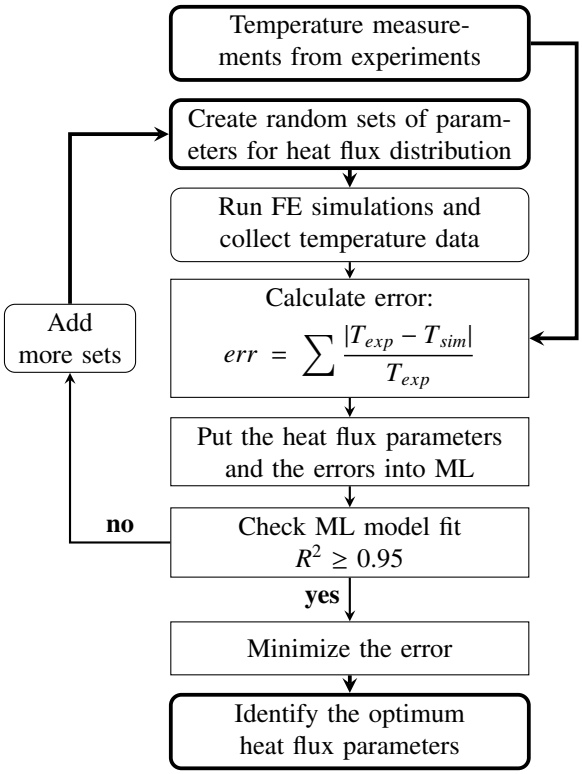

Fig. 1: Flowchart of the ML-based inverse identification process.

2. Inverse Identification Details

2.1. Process of identification

The ML-based inverse approach presented in this study is implemented in MATLAB. The Gaussian process regression with cross-validation, Bayesian optimization and the multiStart minimization algorithm are used to obtain the optimum set of parameters. To build the ML model for the inverse identification process, experimental and simulated temperature data are required to be used as input. The flowchart in Fig. 1 shows the steps followed to build the ML model and to determine the heat flux distribution. The temperature is measured during machining tests at three different locations using embedded thermocouples, the details of which are given in Section 3). In order to describe the heat flux distribution accurately, an equation with 5 parameters is defined (see Section 2.2). Then, the random sets of parameters are created and used as input for heat transfer FE simulations (details are given in Section 4). As soon as the FE simulations are performed, the nodal temperatures are extracted and compared with the experimental temperature measurements at discrete time intervals to calculate the absolute error. The value of the error and the parameters for heat flux distribution are used as input to build the ML model. The coefficient of determination R^2 is monitored to assess the reliability of the trained ML model (i.e., the good fit). If R^2 is not satisfactory, a large set of simulations are performed to enrich the input data and thus the model reliability. When a well-fitted ML model is constructed, a minimization problem is formulated to estimate the optimum set of heat flux distribution parameters, giving the minimum absolute error between the experimental and simulated temperatures. Finally, to validate the results, one more FE simulation is carried out using the optimal heat flux distribution.

2.2. Heat flux distribution equation

The selected equation for the heat flux has 5 different parameters. 4 of them (i.e., b_1 to b_4) represent the distribution on the rake face of the tool, while 1 parameter (i.e., b_5) provides the time-dependency. The distribution of the heat flux on the rake face is given as follows

$$H = \frac{1}{2} + \frac{1}{2}\tanh\Big(a\,(X - b_1)\Big) \tag{1}$$

$$R = Y - b_2 + \frac{(X - b_1)^2}{(AP - b_1)^2}\,b_2\,H \tag{2}$$

$$G = 1 - \frac{X - b_1}{AP - b_1}\,H \tag{3}$$

$$Q = b_3 \exp\left(-\left(\frac{R}{b_4}\right)^2\right) G\,Q_{amp} \tag{4}$$

where H is a smooth approximation to the step function. For bigger values of a, the step function is obtained. R defines the line that follows the maximum heat flux over the rake face while G defines the change in magnitude of the heat flux towards the tool nose. The given equation of G represents the decreasing

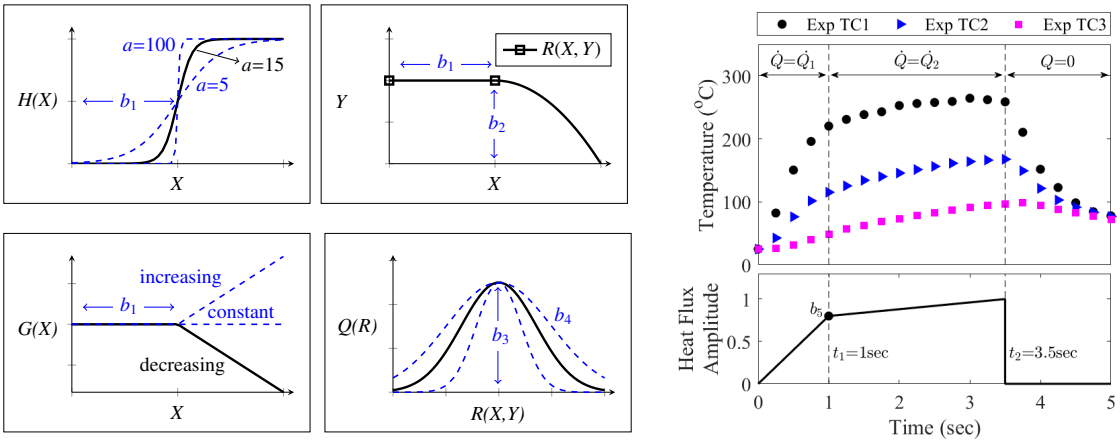

Fig. 2: The representation of heat flux distribution function in 2D (left) and time-dependency of heat flux amplitude Q_{amp} from the temperature measurements for FT2 (right).

heat flux towards the tool nose; however, increasing and constant ones are also investigated based on the temperature distribution obtained from the simulations. The investigation indicates that a constant G represents a more realistic temperature distribution on the rake face compared to increasing and decreasing ones. Finally, Q is the distributed heat flux given in the form of Gaussian distribution, X and Y are coordinates ($\{X,Y\} \in A_c$, rake surface contact area domain), whereas b_1 to b_4 are the parameters to be identified. To see the contribution of the equations further, the outputs of the equations are given in Fig. 2 separately.

The parameter related to time-dependency b_5 represents the change in time in the amplitude of the heat flux Q_{amp}. This change is assumed to be linear and decided based on the experimental temperature data as seen in Fig. 2. This parameter will be also identified with the inverse approach. There are two critical time points in the figure. The time, when the temperature increase changes its behavior (i.e., t_1), is selected as one of the critical points where the amplitude of heat flux changes. At the second point t_2, where the cut ends and the cooling starts, the amplitude of the heat flux is set to zero. It must be noted that the parameters b_1 to b_5 are limited within certain boundaries (based on the depth of cut a_p and the contact length l_c) when creating the random sets of parameters and also during the minimization process. The minimum limits are [a_p/3, l_c/2, 50000, l_c/4, 0.7] while the maximum ones are [a_p–0.3, 9l_c/10, 400000, l_c/2, 1.0] respectively for b_1 to b_5.

3. Temperature Measurement Details

Temperature readings required for the identification process are obtained from the face turning (FT) experiments. These experiments are performed under dry cutting conditions on an EMCO 365 CNC lathe with three different feeds f (0.05, 0.1, 0.15mm/rev) while the cutting speed V_c (150m/min) and depth of cut a_p (0.8mm) are kept constant. Starting from the smallest feed, these cutting conditions are named FT1, FT2 and FT3, respectively. The machined workpiece is C38 steel cylindrical bar with a 156.5mm diameter. The tool (Sandvik Coromant – uncoated cemented carbide CNMA-120404-KR without a chip breaker) and the tool holder (Sandvik Coromant – C3-PCLNR-22040-12) assembly gives 95° major cutting edge angle and 6° rake angle. The machining duration for each cut is kept short (around 4 seconds) to reduce the effect of tool wear on the temperature measurements. Short machining time may result in temperature readings not reaching a steady state. However, since the tool-chip contact area and the chip formation are stable, the heat flux over the contact area will not change significantly over time. Thus, the identification process will not be significantly affected by this short machining duration.

The temperature is measured from three different points during machining (see Fig. 3). Three holes with a diameter of 0.55±0.05mm are produced using electrical discharge machining (EDM) from the bottom of the tools for the thermocouples. The holes are 0.6±0.2mm away from the rake face of the tool in depth. The location and the depth of the thermocouple holes are decided based on preliminary FE simulations to ensure that the temperature measurements at different locations would provide sufficiently large differences required for the model calibration. The thermocouples used in the experiments are mineral insulated thermocouples (Type K) with 0.5mm diameter. A thermal paste is not used in the assembly of thermocouples due to

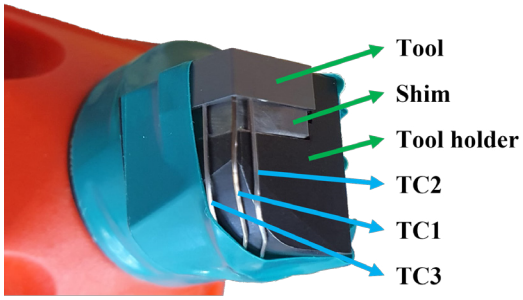

Fig. 3: Experimental setup for temperature measurements with three thermocouples (TC).

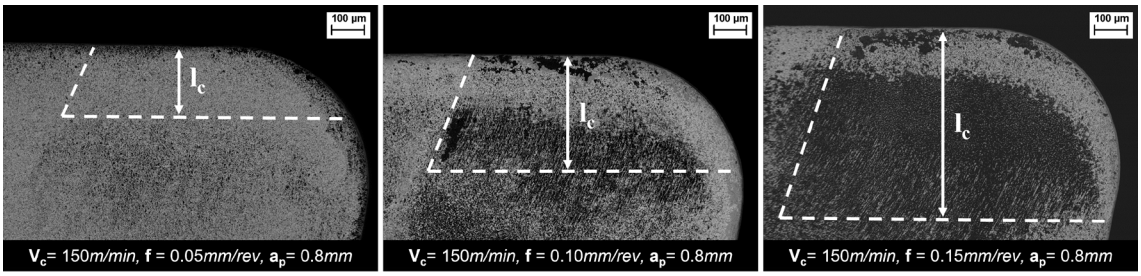

Fig. 4: SEM images of rake face of the tools showing the contact length (l_c) for cutting conditions FT1 (left), FT2 (middle) and FT3 (right).

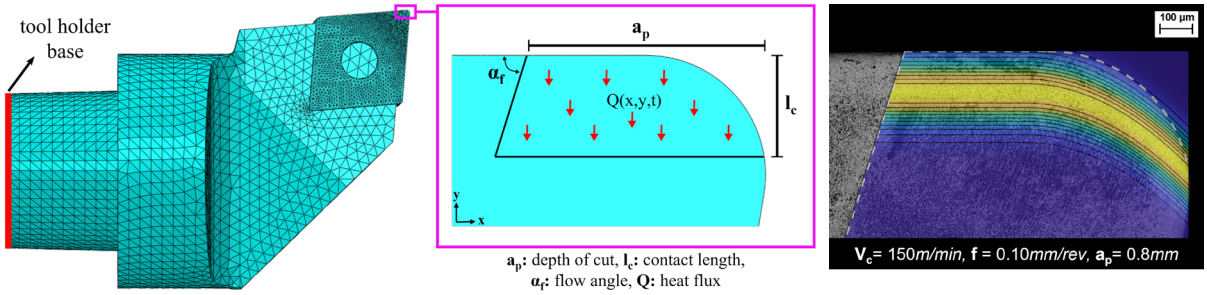

Fig. 5: 3D finite element model (left), tool-chip contact area (middle) and an example heat flux distribution on the contact area (right).

① lack of information about the estimated temperature levels during machining which should be within the operating temperatures of the thermal paste, ② risk of thermal paste filling the tip of the thermocouple holes which may prevent the tool-thermocouple contact at the tip. The readings are collected with a multichannel data logger for synchronized measurements. After the face turning process, the tool-chip contact areas are measured by using Scanning Electron Microscope (SEM) after removing the built-up edge with a diluted HCl solution (see Fig. 4). Then, the position and depth of the holes are re-measured by grinding the flank sides of the tools. A stereo-optical microscope (Zeiss Discovery V20) equipped with image processing software is used for this re-assessment.

4. Heat Transfer Simulation Details

The heat transfer simulations required for the identification process are performed in ABAQUS. The FE models include the components such as the tool, tool holder, shim and thermocouples for a realistic representation of the experimental setup. The material properties used for the components of the FE model are given in Table 1. Perfect contact is considered between the components of the assembly. A constant $25°C$ is also applied at the base of the tool holder as a boundary condition (see Fig. 5). The prescribed heat flux distribution stated in Section 2.2 is applied on the tool-chip contact area which is measured with SEM as mentioned in Section 3. The chip flow angle α_f, which is calculated based on [8], is included in the models to represent a more realistic contact area as seen in Fig 5. The ambient temperature is assumed to be constant $25°C$. The total time of the simulations is selected as 5sec, which includes the air convection cooling part in addition to machining time depending on the value of t_2 (see Fig. 2). The convection coefficient of $0.2kW/m^2K$ (an average value for forced convection of air) is applied on the outer surfaces for the duration of the machining time, then the coefficient is reduced to $0.02kW/m^2K$ (an average value for free convection of air) for the cooling part.

The temperature results from the simulations are collected from the nodes at the top surfaces of the thermocouples, and the average temperature for each thermocouple is calculated. Then, these values are compared with the experimental temperature readings as mentioned in Section 2.1. The number of elements in the FE model is determined carefully considering the computational time and the resolution of the contact area. Since ML requires a large number of data to provide good estimations, it is important to minimize the time per simulation. Moreover, the number of elements in the contact area affects the resolution of the heat flux distribution which is particularly important for the ML model to recognize the effect of each parameter of the heat flux distribution. The assembly consists of 350000 elements, and each simulation takes around 8 minutes on a computer equipped with an Intel(R) Core(TM) i7-8650U CPU @ 1.90GHz 2.11GHz and 16.0GB RAM.

Table 1: Material Properties of the Components of FE-Model

Component	Conductivity (W/mK)	Heat capacity (J/m^3K)
Tool holder	39.6	3.56e+6
Shim	39.6	3.56e+6
Insert	92.9	2.94e+6
Thermocouples	16.1	4e+6

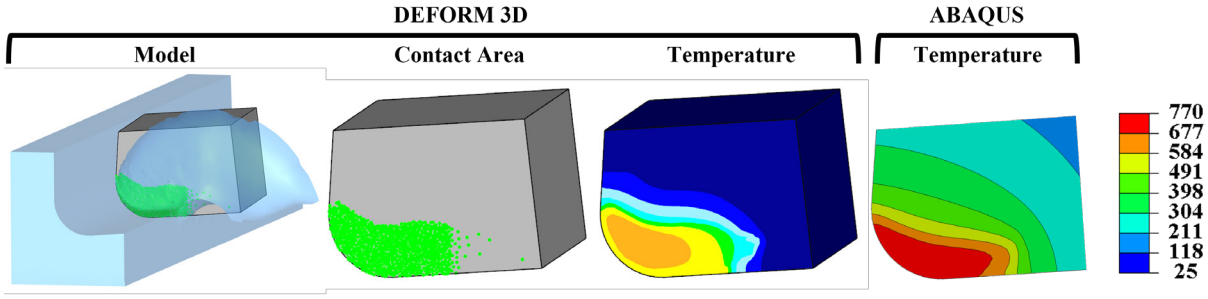

Fig. 6: The DEFORM model setup, contact area and temperature distribution as well as temperature distribution from ABAQUS for FT2.

5. Results and Discussion

A realistic representation of the heat flux distribution should result in a realistic distribution of temperature on the rake face of the tool. Thus, the temperature results from heat transfer simulations (ABAQUS) are compared with the results from machining simulations (SFTC DEFORM 3D) for the cutting condition FT2. The machining FE simulation model is created based on [9]. The machining simulation is performed for 6mm of cut until the cutting forces and the tool-chip contact area reach stable conditions to ensure the heat flux at the tool-chip interface reaches nearly the steady state. The FE model of chip formation, the contact area and temperature distributions are shown in Fig. 6. As can be seen in this figure, the temperature distributions obtained from ABAQUS and DEFORM 3D are similar, although the maximum simulated temperatures differ by about $100°C$. This means that the selected heat distribution equation (Eq. 4) represents the thermal boundary condition at the tool-chip interface appropriately. Moreover, the shape of the contact area is in line with the heat flux distribution shown in Fig. 5. The temperature distribution predicted by ABAQUS is associated with the constant G function (see Fig. 2). Incorporating the G function with ascending or descending behaviours according to (see Fig. 2) can lead to an increase or decrease in heat flux near the tool nose. This alters not only the magnitude of maximum temperature but also the location it occurs on the rake face, i.e. near the tool nose or on the tool face far from the nose. These behaviours are believed to be unrealistic regarding the results of the cutting simulation presented in Fig. 6. Hence a constant G function is chosen for the estimation of heat flux and the temperature distribution on the rake face.

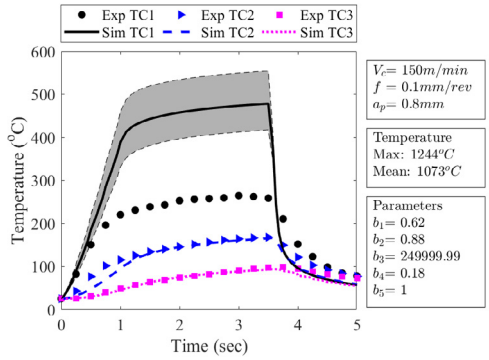

Fig. 7: Identified heat flux distribution parameters and the temperature results for FT2.

The inverse identification of the model parameters is followed according to steps shown in Fig. 1. 200 sets of parameters are randomly generated to achieve a good fit during the training of the ML model for each cutting condition ($R^2 \geq 0.95$). The heat flux distribution parameters (i.e., b_1 to b_5) are then obtained by minimizing the absolute errors calculated from the difference between experimental and simulated temperatures (see 1). It is important to mention that the temperature readings from TC1 are not included in the identification process. As mentioned in the literature [5] and observed in a previous study of ours [6], when the thermocouple is placed very close to the heat source (i.e., tool-chip contact area), the temperature readings show a marked sensitivity with respect to the exact positions of the embedded thermocouples. This is because of the high temperature gradients near the heat source. This phenomenon is demonstrated by the shaded area in Fig. 7, indicating the large influence of a $\pm 200\mu m$ variation in the depth of the fabricated holes for embedding the thermocouple. A $\pm 200\mu m$ variation in the depth of TC2 and TC3 holes showed an insignificant effect on the simulated temperatures. Thus, the error in the identification process (see 1) is calculated based on the readings from TC2 and TC3. As shown in Fig. 7, the ML-based inverse identification approach is capable of estimating the heat flux distribution based on the experimental temperature readings. The simulation results are very close to the experimental values for TC2 and TC3. However, the maximum temperature (given in the figure), is larger than the expected ranges when machining similar materials using uncoated tools, see for example the experimental measurements reported by [10]. Therefore, an additional constraint is imposed during the minimization process, so that the maximum temperature on the rake does not exceed the expected temperature limits reported in the literate. These temperature limits are interpolated using the data reported by [10] when machining carbon steels with cutting speeds ranging from 100-200 m/min and feed ranging from 0.1-0.2 mm/rev. The interpolated maximum temperatures are approximately 680, 760 and $830°C$ for FT1, FT2 and FT3, respectively.

The simulation results after imposing temperature limit constraints during the optimization process are shown in Fig. 8. The obtained maximum temperatures are around the interpolated

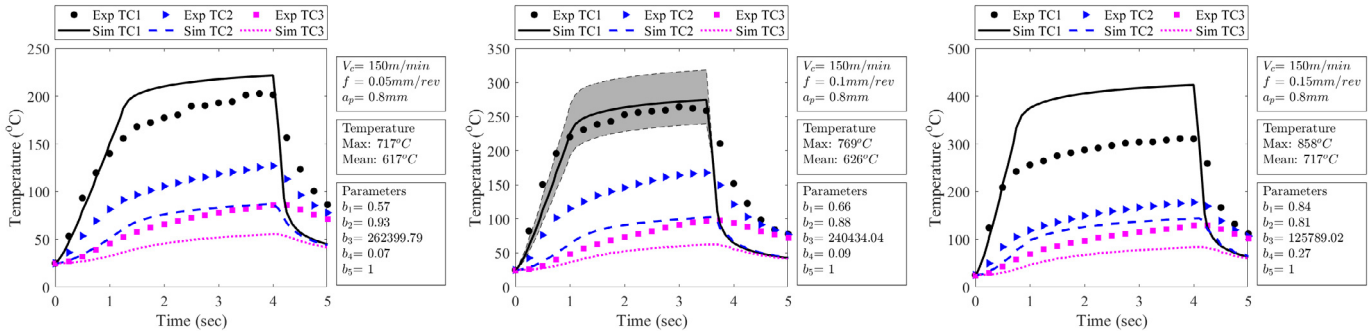

Fig. 8: Identified heat flux distribution parameters and the temperature results for FT1 (left), FT2 (middle) and FT3 (right) after imposing the maximum temperature limit during the optimization process. The shaded region shows the variation in simulated temperature due to a ±200μm variation in depth of the hole.

maximum temperatures. Additionally, the temperature distribution is closer to the ones obtained from DEFORM 3D. In Fig. 6, the maximum temperature in DEFORM 3D is 660°C while it is 770°C in ABAQUS. However, the simulated results in Fig. 8 are not closely in line with the temperature readings obtained from the experiments. This may be due to the experimental difficulties of the temperature measurements during machining. It is almost impossible to know the exact location and the quality of the contact between the thermocouple and the thermocouple hole during machining. Applying a thermal paste may help improve the contact but it can bring other challenges as mentioned earlier in Section 3. The dimensional accuracy of the fabricated holes, in principle, determines the effectiveness of the heat transfer between the tool and the thermocouples and thus it can markedly influence the temperature measurements. Even though the ML-based inverse identification approach has great potential to provide a robust and efficient estimation of the heat flux distribution on the rake face, more reliable temperature measurements are required to enhance the results.

6. Conclusion

In summary, the proposed ML-based inverse approach has a high potential for the identification of the parameters of any given heat flux distribution equation. Compared to previous studies, widening the investigations and including more details such as the time-dependency of the heat flux, changing the magnitude of the heat flux towards the nose radius and more realistic contact area with the effect of flow angle improved the results even further. Additionally, the temperature distribution is investigated and compared with machining simulations. The maximum value of the temperature is also investigated, and later on, another criterion is added to obtain more realistic temperature results. However, to improve the results even further, more reliable experiments are required that ensure the contact between thermocouples and the tool. In this aspect, using measurements from different sources such as grooved thin film thermocouples and thermal cameras may be an alternative approach. Additionally, the other heat sources on the flank surface should be included for a more realistic representation of the machining process.

Acknowledgements

This research was financially supported by the Swedish national research program Vinnova-FFI, project no. 2016-05397. We would also like to acknowledge the support of Chalmers Area of Advance Production, Scania CV, AB Sandvik Coromant and Swedish National Infrastructure for Computing at Chalmers Centre for Computational Science and Engineering.

References

[1] Yvonnet, J., Umbrello, D., Chinesta, F., Micari F., 2006. A simple inverse procedure to determine heat flux on the tool in orthogonal cutting. International Journal of Machine Tools and Manufacture 46, 820–827.
[2] Norouzifard, V., Hamedi, M., 2014. Experimental determination of the tool–chip thermal contact conductance in machining process. International Journal of Machine Tools and Manufacture 84, 45—57.
[3] Brito, R.F., Carvalho, S.R., Lima E Silva, S.M.M., 2015. Experimental investigation of thermal aspects in a cutting tool using comsol and inverse problem. Applied Thermal Engineering 86, 60–68.
[4] Huang, S., Tao, B., Li, J., Fan, Y., Yin, Z., 2018. Estimation of the time and space-dependent heat flux distribution at the tool-chip interface during turning using an inverse method and thin film thermocouples measurement. The International Journal of Advanced Manufacturing Technology 99, 1531—1543.
[5] Kryzhanivskyy, V., Bushlya, V., Gutnichenko, O., M'Saoubi, R., Ståhl, J.E., 2018. Heat Flux in Metal Cutting: Experiment, Model, and Comparative Analysis. International Journal of Machine Tools and Manufacture 134, 81–97.
[6] Erturk, A.S., Malakizadi, A., Larsson, R., 2022. An ML-based approach for inverse identification of heat flux in machining. Procedia CIRP 115, 208–213.
[7] Li, X., Kopalinsky, E.M., Oxley, P.L.B., 1995. A Numerical Method for Determining Temperature Distributions in Machining with Coolant Part 2: Calculation Method and Results. Proceedings of the Institution of Mechanical Engineers Part B: Journal of Engineering Manufacture 209, 45–52.
[8] Arsecularatne, J.A., Mathew, P., Oxley, P.L.B., 1995. Prediction of Chip Flow Direction and Cutting Forces in Oblique Machining with Nose Radius Tools. Proceedings of the Institution of Mechanical Engineers, Part B: Journal of Engineering Manufacture 209, 305–315.
[9] Erturk, A.S., Malakizadi, A., Larsson, R., 2020. A thermomechanically motivated approach for identification of flow stress properties in metal cutting. The International Journal of Advanced Manufacturing Technology 111, 1055-–1068.
[10] Saez-de-Buruaga, M., Soler, D., Aristimuno, P.X., Esnaola, J.A., Arrazola, P.J., 2018. Determining tool/chip temperatures from thermography measurements in metal cutting. Applied Thermal Engineering 145, 305-–314.